Estimating time-dependent solar gains through opaque building envelope parts: an explorative study on a test box

Xiang Zhang[1,2]***, Dorit Aviv**[1]**, Dirk Saelens**[2,3] **and Staf Roels**[2]

[1] University of Pennsylvania, Weitzman School of Design, Thermal Architecture Lab, 210 South 34th Street Philadelphia, PA, USA
[2] KU Leuven, Department of Civil Engineering, Building Physics and Sustainable Design Section, Kasteelpark Arenberg 40 Bus 2447, 3001 Heverlee, Belgium
[3] EnergyVille, Thor Park 8310, BE-3600 Genk, Belgium

*Corresponding email: jaxzhang@upenn.edu; jason.zhang.kul@outlook.com

Abstract. Accurate estimation of the energy gain from solar radiation in buildings is necessary for building energy performance characterization, model predictive control (MPC), fault detection and diagnostics, etc. Solar radiation affects the buildings' internal air temperature dynamics, either (directly) by penetrating the glazing or (indirectly) through the opaque building envelope. Nevertheless, no research has investigated the on-site data-driven modelling of the indirect effects of solar radiation i.e., additional solar gain through the opaque building envelope, marked as indirect solar gain. Therefore, this work aims to develop grey-box model-based techniques to characterize the dynamics of indirect solar gain. A test box, with overall dimensions of 120*120*120 cm^3, that represents a simplified scale model of a building is examined, to provide an initial understanding of this matter. This test box is south-north orientated and has only one window of 60*60 cm^2, positioned on its southern wall. On-site data associated with this text box was recorded during the summer (June-July) in Almeria, Spain. This simplified reduced-size text box satisfies the research goal very well to serve as a pilot case study, since the indirect solar gain was the dominant effect of solar radiation. Based on the in-situ data from this case, a three-dimensionally decomposed solar irradiance integrated grey-box modelling technique is proposed for characterizing the dynamics of indirect solar gain. Preliminary results from this study show that this technique can effectively reveal the key dynamics of indirect solar gain and outperform the classic grey-box model, based on limited low-frequency on-site measured data.

Keyword. On-site data; grey-box model; B-splines; solar radiation spatial decomposition; solar gain; opaque building envelope

1. Introduction

1.1. Solar gains in buildings

The indoor thermal dynamics of buildings are influenced by outdoor solar radiation [1–4]. This impact is generally referred to as a specific energy gain - solar gain (*Sg*). Various energy gains and losses, including solar gain, heating gain from heating systems, internal heat from occupants and appliances, heat transmission, ventilation, and infiltration, determine the indoor thermal dynamics. Therefore, to model the interior thermal dynamics in buildings accurately, it is crucial to measure or estimate the data of dynamic solar gain precisely. In building physics, solar gain is generally categorized into two parts: direct and indirect gains [5], based on different heat transfer mechanisms. In literature, studies on solar gains in buildings predominantly emphasize the part of solar gain penetrating the glazed envelope [6] (Sg_{gla}), while giving limited consideration to the other part [7] (Sg_{opa}). This focus may be appropriate for well-insulated buildings with a high window-to-wall ratio (WWR), where Sg_{opa} is much less significant in comparison to Sg_{gla}. However, in most buildings, especially the ones with poor insulation and low WWR, Sg_{opa} can be a vital part. This is mainly attributed to the large exterior surface area of opaque envelopes in buildings, such as walls and roofs. For example, a WWR between 0.2 and 0.4 is a typical range for most buildings [8]. This range suggests that the opaque building envelope makes up between 60% and 80% of the total exposed exterior surface area in most buildings. To address this gap, this study selects a test box case with limited impacts of Sg_{gla} to focus on investigating Sg_{opa}. On-site measured data of a case study will be used in data-driven modelling of solar gains, which pass through the glazed envelope and opaque envelope. The next section introduces the applied statistical modelling technique. Section 1.3 will present the case study.

1.2. On-site data-driven statistical modellings

Using statistical modelling to analyse on-site data of buildings is a growing trend for both estimating and predictive controlling the energy performance of buildings [9]. There are three main types of modelling: white-, grey-, and black-box models. The grey-box model combines the benefits of both white-box (based solely on physical knowledge and equations) and black-box (entirely data-driven) models [10–13]. Hence, most parameters of the grey-box model are physically interpretable, which matches with the aim of this study in estimating dynamic Sg_{opa}. To provide an example, the simplest grey-box model of a building can be represented mathematically by Eqs. (1-2) and Figure 1. This model simplifies the building to a single thermal zone and represents it as a one-state RC network model. The readers refer to [10,12] for the interpretations of Eqs. (1-2). For instance, in Eq. (1), *Sg* is interpreted as the sum of both Sg_{gla} and Sg_{opa} physically, as shown in Eq. (3). T_i and T_a stand for the indoor and ambient temperature, while R_{ia} represents the thermal resistance against heat flux between them. ϕ_h denotes the energy flux supplied by the heating system. C_i and C_e indicate the heat capacities of interior air mass and the building envelope respectively. $\{\omega_i,t\}$ and $\{\omega_e,t\}$ represent independent standard Wiener processes. The incremental variances of the Wiener processes are marked as σ_i^2 and σ_e^2.

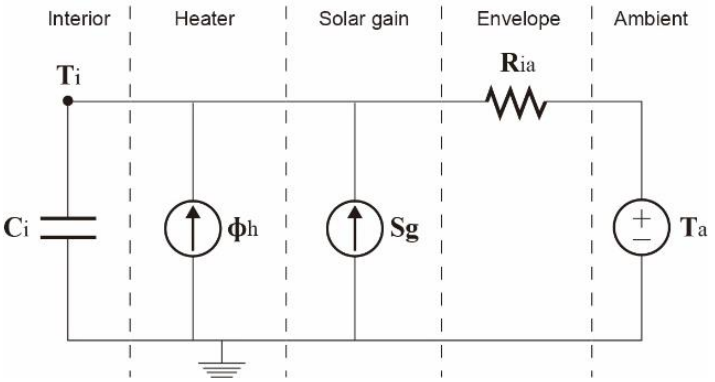

Figure 1. One-state single-zone RC-network model of a building's thermal dynamics [14]

$$dT_i = (\frac{1}{R_{ia}C_i}(T_e - T_i) + \frac{1}{C_i}(Sg + \phi_h))d_t + \sigma_i d\omega_i \quad (1)$$

$$Y_k = T_{ik} + e_k \quad (2)$$

It is noted that Sg, ϕ_h and etc., in Eq. (1), are time dependent. As shown in Eq. (3), the total dynamic solar gain Sg_t is typically estimated via a product of solar aperture (gA) and measured global horizontal irradiance (GHI_t). The gA-value (in m^2), also called the solar gain factor or effective window area, is generally defined as the equivalent area of a perfectly transparent surface that allows the same amount of solar radiation energy to penetrate the building's interior environment through either glazed or opaque building envelope [15]. In addition, GHI_t (W/m^2) composes of both diffuse and direct solar radiation, which are commonly measured as diffuse horizontal irradiance (DHI_t) (W/m^2) and direct normal irradiance (DNI_t) (W/m^2) respectively, in practice. The transformation of both DHI_t and DNI_t to GHI_t follows Eq. (4), where θ_s indicates the zenith angle of the sun. Therefore, both $Sg_{gla,t}$ and $Sg_{opa,t}$ consists of corresponding diffuse and direct parts, contributed by diffuse (e.g., *DHI*) and direct solar radiation (e.g., *DNI*), which are marked as $Sg_{gla,dif,t}$, $Sg_{gla,dir,t}$, $Sg_{opa,dif,t}$, and $Sg_{opa,dir,t}$ respectively. In this classification, the total solar gain is composed of the said four parts, as shown in Eq. (3). In addition, similar formulations of solar gain estimation to $Sg_t = gA\ GHI_t$ can also be written for each solar gain part among the four, such as Eqs. (5-6) used to estimate $Sg_{opa,dif,t}$ and $Sg_{opa,dir,t}$, based on corresponding customized solar gain coefficients: $gA_{opa,dif}$ and $gA_{opa,dir}$.

$$Sg_t = gA\ GHI_t = Sg_{gla,t} + Sg_{opa,t} = Sg_{gla,dif,t} + Sg_{gla,dir,t} + Sg_{opa,dif,t} + Sg_{opa,dir,t} \quad (3)$$

$$GHI_t = DHI_t + DNI_t \cos\theta_{s,t} \quad (4)$$

$$Sg_{opa,dif,t} = gA_{opa,dif} DHI_t \quad (5)$$

$$Sg_{opa,dir,t} = gA_{opa,dir} DNI_t \quad (6)$$

2. A test box as case study

In this study, a test box representing a scale model of a simplified building is investigated, as an explorative case study. The datasets were collected in the summer from 28 June to 01 July 2013 in Spain within the framework of the IEA-EBC Annex-58 project. For more details of the test box of the Annex-58 project, the readers refer to [4,16]. In brief, the test box is in a cubic form with all building fabrics identical in material, construction, and thickness (i.e., 12 cm), including walls, floor, and ceiling. The exterior and interior dimensions of the box are 120*120*120 cm^3 and 96*96*96 cm^3. Only one window component is included in the southern wall of the test box, in 60*60 cm^2 with a glazed part of 52*52 cm^2. The test box was south-north orientated on the premises of CIEMAT in Almeria, Spain (Lat. 37°6′ N, Long. 2°24′ W). A Randomly Ordered Logarithmic Binary Sequence of heat inputs (ROLBS) heating signal was imposed during the measurement campaign. For the details of measurement campaigns, the reader may refer to [17], pages 55-77 (CIEMAT case), and the images of measurement campaigns are shown in Figure 2. In line with [14,18], only indoor temperature (°C), outdoor temperature (°C), heating input (W), global horizontal irradiance (*GHI*) (W/m^2), direct normal irradiance (*DNI*) (W/m^2), and diffuse horizontal irradiance (*DHI*) (W/m^2), and wind speed (m/s) are included in the dataset, which is re-sampled from original 5 mins sampling time into a 20 mins frequency. The indoor temperature and heating input (in the ROBLS test) are measured in the box and the rest of the input weather data are recorded in a weather station on site [17]. It is noted that only *GHI* and *DHI* are measured directly, while *DNI* is converted via Eq. (7) indirectly, a deformation of Eq. (4). In practice, the corresponding $\theta_{s,t}$ data for the specific periods is generated in R by package 'maps' (version 3.4.0) and package 'GeoLight' (version 2.0.0) based on longitude and latitude data.

Figure 2. Image of the test box on which a ROLBS heating measurement campaigns was performed at CIEMAT, Spain [17]

$$DNI_t = \frac{GHI_t - DHI_t}{\cos\theta_{s,t}} \tag{7}$$

One of the reasons for selecting this test case, as an explorative study, is attributed to the strong solar irradiance in Spain during the summer, which makes it suitable for investigating solar gains. Most importantly, as mentioned in section 1.1, the Sg_{gla} theoretically has minimal impact in this case, which aligns with the research focus on Sg_{opa} in this study. Specifically, the small glazing size in the test box (0.27 m^2) allows only a slight amount of diffuse irradiance to pass through, resulting in a limited amount of $Sg_{gla,dif,t}$. Additionally, the 'high' summer sun's path in Southern Spain makes the corresponding $Sg_{gla,dir,t}$ is almost negligible. Specifically, Figure 3 visualizes the relationship between the test box and the daily sun's trajectory on 01 July 2013, based on the said dimensional data of the test box and the sun's path information from [19] (e.g., sunrise, sunset, and daylength). As shown in Figure 3, direct normal irradiance (DNI_t) falls less than three hours, from 12:49 to 15:37, on the window glazing. In addition, during this time, the solar altitude varies from 67 to 76 degrees, resulting in ignorable $Sg_{gla,dir,t}$. The constructed 20 mins sampled dataset is visualized in Figure 4.

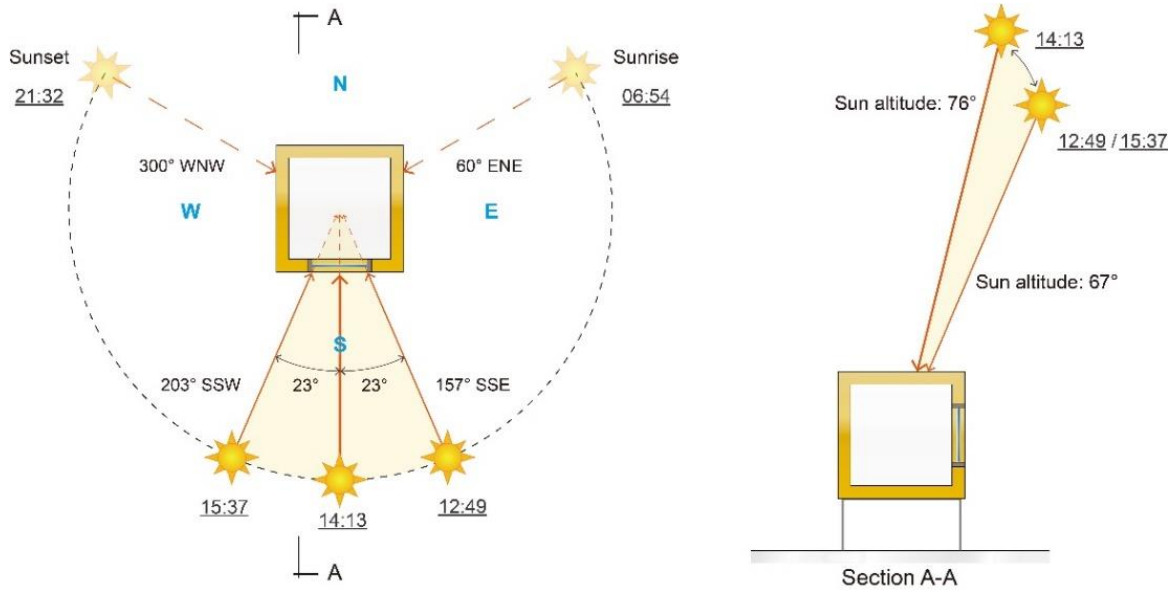

Figure 3. The analysis on the relationship between the test box and the sun trajectory on 01 July 2013.

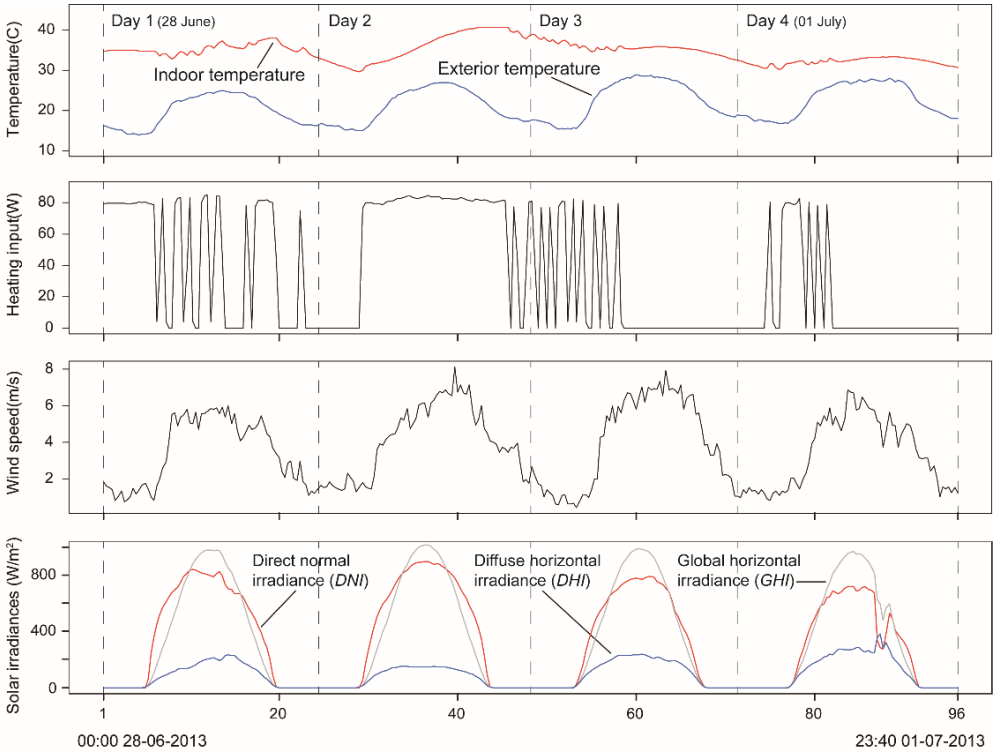

Figure 4. The visualization of 4-day dataset used in this study.

3. Three-dimensional pre-decomposed *DNI* based grey-box modelling

3.1. Three-dimensional pre-decomposition of DNI

As clarified in section 2, the data of DNI_t can be calculated via Eq. (7) based on measured GHI_t and DHI_t and the corresponding θ_s data. Moreover, as shown in Figure 5, it is possible to pre-decompose DNI_t data three-dimensionally, into $DNI_{x,t}$, $DNI_{y,t}$ and $DNI_{z,t}$, based on corresponding θ_s and solar azimuth φ_s data and simple trigonometric calculations. In practice, similar to θ_s, the required φ_s data is also calculated in R by package 'maptools' (version 1.1-6) with longitude and latitude data. Therefore, the DNI_t data is three-dimensionally pre-decomposed into five parts, which are perpendicular to five envelope surfaces of the south-north orientated cubic test box: roof, east, south, west, and north walls corresponding, marked as $DNI_{r,t}$, $DNI_{e,t}$, $DNI_{s,t}$, $DNI_{w,t}$ and $DNI_{n,t}$ and visualized in Figure 6. It is noted that $DNI_{r,t} = DNI_{z,t} = GHI_t - DHI_t$, which is also known as direct horizontal irradiance.

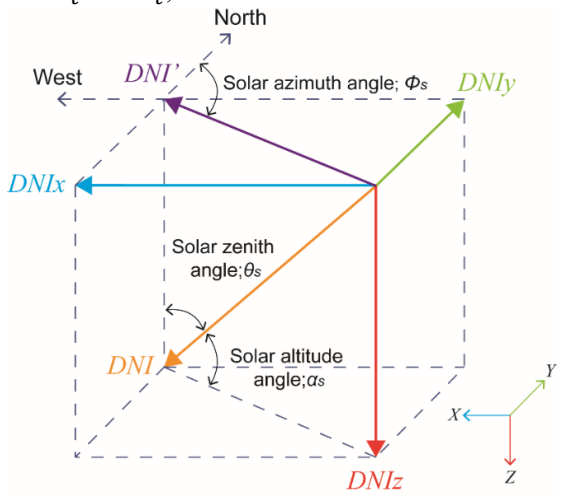

Figure 5. The diagram of three-dimensional decomposition of direct normal irradiance (*DNI*).

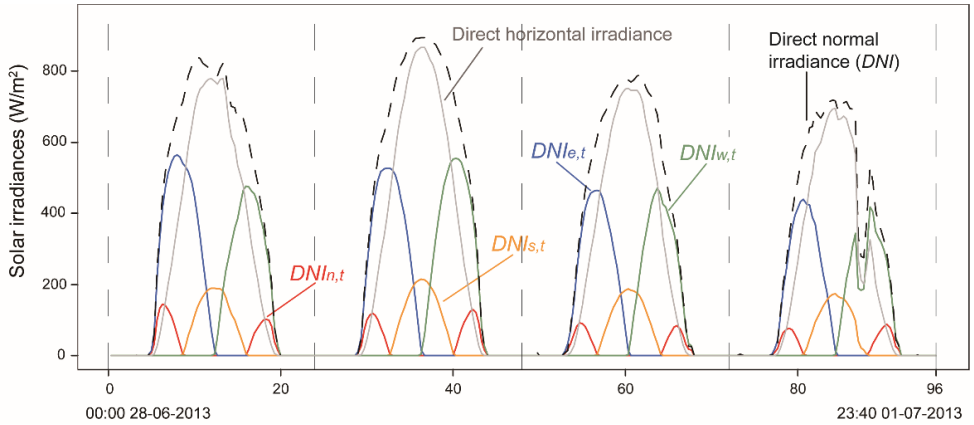

Figure 6. The diagram of three-dimensional decomposition of direct normal irradiance (*DNI*).

Based on the pre-decomposed DNI_t, Eq. (6) Equation (6) can be further expanded into Eq. (8) by assigning customized solar gain coefficients for $DNI_{r,t}$, $DNI_{e,t}$, $DNI_{s,t}$, $DNI_{w,t}$ and $DNI_{n,t}$ respectively, such as gA_r for roof and gA_s for south wall. As mentioned in section 2, the cubic test box has identical size, material, construction and thickness in the roof, east, west and north walls. Therefore, it is reasonable to assume $gA_r = gA_e = gA_w = gA_n$ to reduce the number of parameters in the followed grey-box modelling. In addition, the Eq. (8) based grey-box model will be marked with suffix "*_deco*".

$$Sg_{opa,dir,t} = gA_r DNI_{r,t} + gA_e DNI_{e,t} + gA_s DNI_{s,t} + gA_w DNI_{w,t} + gA_n DNI_{n,t} \quad (8)$$

3.2. Forward selection of grey-box models

Forward model selection is used in identifying a suitable grey-box model, the readers refer [10,14] for more details. Figure 7 shows the process of forward model selection in this study. The suffix "*_Aopa*" indicates the Sg_{gla} and Sg_{opa} are modelled in the system equations of grey-box model separately and Sg_{opa} is simplified as a lumped one, while suffix "*_deco*" represents the model elaborates Sg_{opa} modelling based on Eq. (8). The system equations of *TiTe_deco* model is written as Eqs. (9-10), based on the estimated gA_r and gA_s values, the daily dynamic $gA_{opa,dir,t}$ curve is estimated via Eq. (11), as a deformed formula of Eq. (6) and Eq. (8). $gA_{gla}GHI$ represents the sum of $Sg_{gla,dif}$ and $Sg_{gla,dir}$. In addition, $Sg_{opa,dif}$ and $Sg_{opa,dir}$ are calculated via Eq. (5) and Eq. (8).

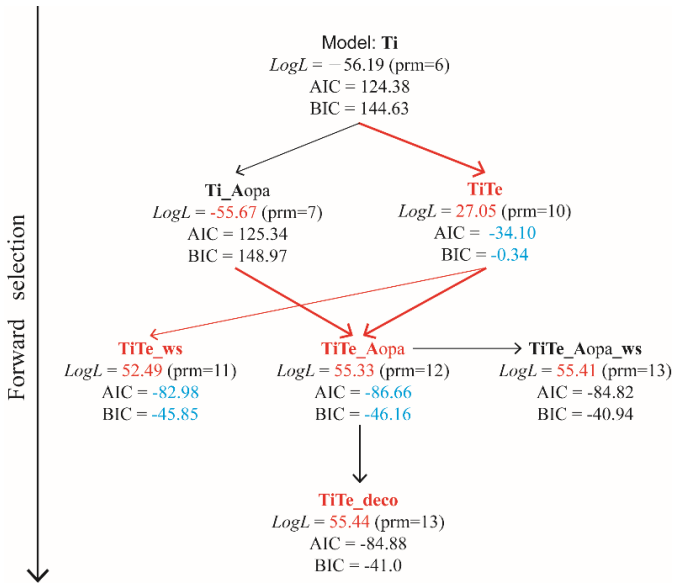

Figure 7. Forward model selection of grey-box models in this study.

$$dT_i = \left(\frac{1}{R_{ie}C_i}(T_e - T_i) + \frac{1}{C_i}(gA_{gla}GHI + \phi_h)\right)dt + \sigma_i d\omega_i \quad (9)$$

$$dT_e = \left(\frac{1}{R_{ie}C_e}(T_i - T_e) + \frac{1}{R_{ea}C_e}(T_a - T_e) + \frac{1}{C_e}(gA_{opa,dif}DHI + gA_r(DNI_{r,t} + DNI_{e,t} + DNI_{w,t} + DNI_{n,t}) + gA_sDNI_{s,t})\right)dt + \sigma_e d\omega_e \quad (10)$$

$$gA_{opa,dir,t} = \frac{gA_r(DNI_{r,t} + DNI_{e,t} + DNI_{w,t} + DNI_{n,t}) + gA_sDNI_{s,t}}{DNI_t} \quad (11)$$

4. Outcomes and conclusion

The estimation outcomes of *TiTe_Aopa* (i.e., 0.034) and *TiTe_deco* models (the red curve) are shown and compared in Figure 8. It is noteworthy that although elaborating the modelling of $Sg_{opa,dir,t}$ dynamics did not result in a significant statistical improvement (i.e., from 55.33 to 55.44 in Loglikelihood) from *TiTe_Aopa* to *TiTe_deco* models, the three-dimensional de-composed DNI_t integrated grey-box model (i.e., *TiTe_deco* model) can accurately characterize the key dynamics of $gA_{opa,dir,t}$. In brief, two 'mirrored' $gA_{opa,dir,t}$ are expected when the sun is positioned around 135º SE and 225 º SW, when DNI_t falls on the largest joint area of the opaque envelope on the roof, south wall, and east wall (or west wall). Between the two peaks, a low value of $gA_{opa,dir,t}$ is expected to occur when only the roof and south wall of the test box are exposed to DNI_t. Comparing the white-box model simulation of $gA_{opa,dir,t}$ (e.g., Energyplus-based) with the estimation outcomes of the grey-box model is interesting future work. Figure 9 compares the estimated daily $Sg_{opa,dir,t}$ dynamic estimated by *TiTe_Aopa* model (with constant $gA_{opa,dir}$) and *TiTe_deco* model integrated dynamic $gA_{opa,dir,t}$. At this stage, without the reference $Sg_{opa,dir,t}$ data, it is hard to determine which model under- or over-estimate $Sg_{opa,dir,t}$. However, it is clear that, the constant $gA_{opa,dir}$ based *TiTe_Aopa* model can not characterize the expected local dynamics of $Sg_{opa,dir,t}$ above-mentioned, such a relative significant $Sg_{opa,dir,t}$ value drop around the noon.

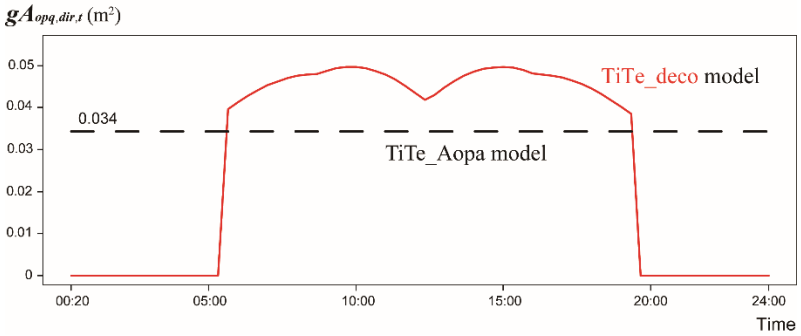

Figure 8. Constant $gA_{opa,dir}$ value and daily dynamic $gA_{opa,dir,t}$ curve estimated by *TiTe_Aopa* and *TiTe_deco* models respectively.

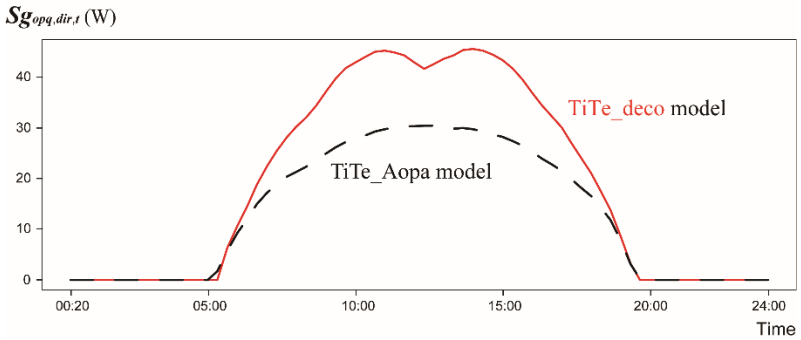

Figure 9. Daily dynamic $Sg_{opa,dir,t}$ estimated by *TiTe_Aopa* and *TiTe_deco* models respectively.

The more realistic information of dynamic solar gain, estimated by the updated grey-box modeling technique proposed in this study, will be beneficial to enhance the performances of most predictive applications of indoor thermal dynamics, such as indoor temperature predictive and model predictive control (MPC), to facilitate building energy reduction and comfort improvement.

References

[1] G. Bauwens, K. Ritosa, S. Roels, J. Deltour, G. Masy, M. Senave, X. Zhang, C. Rasmussen, R. Simon, S. Kristian, EBC Annex 71: Building Energy Performance Assessment Based on In-situ Measurements:Physical Parameter Identification, Leuven, 2021.

[2] Y.B. Yoon, D.S. Kim, K.H. Lee, Detailed heat balance analysis of the thermal load variations depending on the blind location and glazing type, Energy Build. 75 (2014) 84–95.

[3] J. Conejo-Fernández, F. Cappelletti, A. Gasparella, Including the effect of solar radiation in dynamic indoor thermal comfort indices, Renew. Energy. 165 (2021) 151–161.

[4] H. Madsen, P. Bacher, G. Bauwens, A.H. Deconinck, G. Reynders, S. Roels, E. Himpe, G. Lethé, IEA EBC Annex 58: Report of Subtask 3, part 2: Thermal performance characterisation using time series data – statistical guidelines, 2016.

[5] H. Hens, Heat transfer, Build. Phys. - Heat, Air Moisture. (2017) 15–124.

[6] J.L. Wright, C.S. Barnaby, M.R. Collins, N.A. Kotey, Solar Gain through Windows with Shading Devices: Simulation Versus Measurement, (2009).

[7] F. Ascione, L. Bellia, P. Mazzei, F. Minichiello, Solar gain and building envelope: The surface factor, Build. Res. Inf. 38 (2010) 187–205.

[8] K. Javad, G. Navid, Thermal comfort investigation of stratified indoor environment in displacement ventilation: Climate-adaptive building with smart windows, Sustain. Cities Soc. 46 (2019) 101354.

[9] IEA(International Energy Agency), ANNEX 71- Building Energy Performance Assessment Based on In-situ Measurements, (2021). https://iea-ebc.org/projects/project?AnnexID=71.

[10] P. Bacher, H. Madsen, Identifying suitable models for the heat dynamics of buildings, Energy Build. (2011).

[11] A.H. Deconinck, S. Roels, Comparison of characterisation methods determining the thermal resistance of building components from onsite measurements, Energy Build. (2016).

[12] X. Zhang, K. Ritosa, D. Saelens, S. Roels, Comparing statistical modeling techniques for heat loss coefficient estimation using in-situ data, J. Phys. Conf. Ser. 2069 (2021) 12101.

[13] X. Zhang, D. Saelens, S. Roels, Data-driven estimation of time-dependent solar gain coefficient in a two-zone building with synthetic occupants: Two B-splines integrated grey-box modeling approaches, Build. Environ. (2023) 110311.

[14] X. Zhang, C. Rasmussen, D. Saelens, S. Roels, Time-dependent solar aperture estimation of a building: Comparing grey-box and white-box approaches, Renew. Sustain. Energy Rev. 161 (2022) 112337.

[15] X. Zhang, In-situ Data-driven Estimation of Dynamic Solar Gains in Buildings: Grey- and Black- box Approaches, KU Leuven, 2023.

[16] S. Roels, P. Bacher, G. Bauwens, S. Castaño, M.J. Jiménez, H. Madsen, On site characterisation of the overall heat loss coefficient: Comparison of different assessment methods by a blind validation exercise on a round robin test box, Energy Build. (2017).

[17] M.J. Jiménez, IEA EBC Annex 58: Report of Subtask 3, part 1: Thermal performance characterization based on full scale testing: description of the common exercises and physical guidelines, 2016.

[18] X. Zhang, D. Saelens, S. Roels, Estimating dynamic solar gains from on-site measured data: An ARX modelling approach, Appl. Energy. 321 (2022) 119278.

[19] Almería, Almería, Spain — Sunrise, Sunset, and Daylength, July 2013, (2023). https://www.timeanddate.com/sun/spain/almeria?month=7&year=2013 (accessed February 1, 2023).